

Modeling of post-surgical brain and skull defects in the EEG inverse problem with the boundary element method

C.G. Bénar, J. Gotman*

*Department of Neurology and Neurosurgery, Montreal Neurological Institute, McGill University,
3801 University Street, Montreal, Quebec, Canada H3A 2B4*

Accepted 30 October 2001

Abstract

Objectives: In order to obtain accurate EEG inverse solutions in patients subjected to surgery, we have studied the feasibility and influence of incorporating brain and skull defects in realistic head models.

Methods: We first measured the conductivity of the methacrylate used for cranioplasty. Then, we designed realistic boundary element method head models with a skull burr hole, a methacrylate plug or a temporal-lobe resection. We simulated the potentials that would be produced at 71 electrode locations (10/10 system) by dipoles located near the defects. Then, we fitted dipoles on these potentials using a defect-free head model. We also ran simulations in a noisy situation and with higher skull and cerebrospinal fluid (CSF) conductivity.

Results: The largest errors were found for burr holes, with a localization error up to 20 mm for a radial dipole located 30 mm below the hole and an amplification factor of 8. Methacrylate plugs lead to errors up to 5 mm and 0.5; the resection only lead to errors of 2 mm and 1.3. Results obtained with noise were consistent with those obtained without noise. Doubling the skull conductivity led to errors that were reduced by 10–20%, while doubling CSF conductivity increased the errors by up to 31%.

Conclusions: We have shown that it is important to incorporate skull defects in realistic head models when sources are located near the defects and precision is sought. Brain cavities of the size of a typical anterior temporal lobe resection may be omitted without a significant impact on dipole localization. © 2002 Elsevier Science Ireland Ltd. All rights reserved.

Keywords: Realistic head modeling; EEG source localization; Skull defects; Boundary element method

1. Introduction

Techniques solving the inverse problem of electroencephalography (EEG) can be used in an attempt to localize generators of brain activity such as evoked potentials or epileptic spikes. These methods use the theory of electromagnetic fields in order to calculate the potential distribution that is generated at the surface of a volume conductor by internal current sources. They need a model of neuronal activity as well as a mathematical representation of the head that takes into account the different tissue conductivities. Indeed, the electrical activity of a limited area of cortex can be represented as that of a current dipole inside a volume conductor (Nunez, 1981). A classical head model comprises a set of concentric spheres representing the brain, skull and skin interfaces (Rush and Driscoll, 1969; Kavanagh et al., 1978). A more recent approach makes use of a ‘realistic head model’ consisting of meshes of discreet

elements based on real anatomical data. In the boundary element method (BEM, Barnard et al., 1967; Hämäläinen and Sarvas, 1989; Meijs et al., 1989), only boundary surfaces are tessellated, while in the finite element method (FEM, Yan et al., 1991) the whole head volume is meshed. The FEM can represent more heterogeneous configurations than the BEM and can take into account anisotropy (Marin et al., 1998), but is more demanding computationally.

Patients who have undergone brain surgery challenge head modeling techniques, presenting skull and brain defects that affect the conduction of electrical currents. However, source reconstruction may be needed for patients who are not seizure-free after the surgical removal of an epileptogenic lesion. We, therefore, propose in this study to investigate the feasibility and effectiveness of accounting for post-surgical defects in dipole modeling. We will limit ourselves to the BEM.

2. Epilepsy surgery and its effects on the EEG

In a standard procedure of brain surgery, burr holes of

* Corresponding author. Tel.: +1-514-398-1953; fax: +1-514-398-8106.
E-mail address: jgotma@mni.mcgill.ca (J. Gotman).

approximately 10 mm in diameter are drilled into the skull as a first step in the removal of the bone flap. During surgery, parts of the brain are resected, leaving a space that will be filled later with cerebrospinal fluid (CSF) (for a description of temporal lobectomy, see Olivier, 1987). At the end of the surgical procedure, burr holes are filled with a methacrylate-based paste, except one that is left open for drainage. In the period following the operation, the open burr hole fills naturally with soft tissue, which creates a path of least electrical resistance through the skull. We address here 3 types of defects: open burr holes, methacrylate plugs and brain resections. Whereas the resistivity of CSF and soft tissue is known, that of the methacrylate-based substance used in brain surgery has not to our knowledge been published. We present here a test of the electrical properties of this substance.

The fact that skull defects have a large effect on the EEG has been known from the beginning of EEG (Berger, 1969). Cobb et al. (1979) used the word ‘breach rhythm’ for the mu-like activity that can arise close to skull holes; they also reported an enhancement of the amplitude of alpha and frontal fast rhythms ‘over or near unilateral posterior and frontal defects, respectively’. Thevenet et al. (1992) studied the effect of a large hole in the skull on the localization of tangential dipoles in a 3-sphere FEM model. They placed tangential dipoles in a sphere with a hole and fitted dipoles on the resulting potential without taking the hole into account. They found that the recovered dipoles were closer to the hole, and that ‘the closer the dipole is from the hole (or turn towards it), the more important is the error’. Cuffin (1993) has done a similar type of study, with local variations in the thickness of the skull and scalp layers. In the case of a depression in the skull-scalp surface, he found a localization error of about 5 mm and an amplification factor of about 1.2 for a radial dipole 10 mm below the skull. van den Broek et al. (1998) modeled holes of about 20 mm in diameter in a FEM realistic head model. They quantified the effect of the holes on the scalp potential with the relative-difference measure (RDM). They found the largest influence for a radial dipole located just below the hole, which resulted in an RDM of 600%. It is also interesting to note that they found an influence of hole location. Ollikainen et al. (1999) studied the influence on dipole models of an inhomogeneity with a radius of 5 mm and small conductivity. They generated scalp potentials in the model with the inhomogeneity, added noise to the simulated potentials and fitted a dipole onto the result. For 64 electrodes, they found a mean localization error of about 3.5 mm with the non-uniform model and about 10 mm with the uniform model. The error in magnitude was 9 and 19%, respectively. van Burik and Peters (2000a) injected currents in intracerebral electrodes in order to create artificial current dipoles. Dipole models were then fitted on the data, with a fixed location and orientation corresponding to the true ones. Different head models were used, with or without the two trephine holes of diameter 23 mm and their bone plugs. They found that

potential maps were greatly distorted by holes, even for deep sources. Vanrumste et al. (2000) studied the impact of omitting a hole of diameter 20 mm on dipole localization. They used simulations and the finite difference method, and found errors up to 5.2 mm in a 53-electrode setting.

The influence of CSF cavities or zones of low conductivity like methacrylate plugs are less documented. van den Broek et al. (1998) found that inclusion of the ventricles in the head model had a large effect on the RDM for dipoles within a few centimeters of these cavities. Also, dipoles located behind a zone of very low conductivity inside the brain could present an RDM as low as 10%. Vanrumste et al. (2000) found that neglecting the ventricular system could lead to errors of up to 6.1 mm for dipoles in its vicinity.

We can infer from the results presented above that post-operative defects are likely to have an influence on dipole modeling for sources located near the defects. It is, however, not totally clear how large is the brain area influenced by a typical burr hole of a diameter of 10 mm. There is also a need in our clinically oriented approach to study the influence of burr holes filled with methacrylate or of an extended brain resection. We will first present our measurements on the resistivity of methacrylate, then the main study.

3. Measurement of methacrylate resistivity

3.1. Method

We built a $4.9 \times 4.9 \times 0.2$ cm³ plate of methacrylate (Howmedica International Inc., Ireland) and placed it in the center of a $9.8 \times 4.9 \times 4.9$ cm³ container, thereby dividing it into two equal parts. The edges of the plate were sealed using a silicone gel. The two parts of the container were filled with a solution of artificial CSF (aCSF) in order to simulate physiological conditions. One circular electrode of diameter 2.5 cm was placed at each end of the container. We then measured the resistance and capacity of the system, as well as those of the container with aCSF alone. The meter used was a Hewlett Packard 4261A LCR, set at a frequency of 1 kHz. The resistivity ρ_{acryl} ($\Omega \cdot \text{cm}$) of the plate was calculated as:

$$\rho_{\text{acryl}} = \frac{R_{\text{meas}} \text{Surf}}{l} \quad (1)$$

where R_{meas} (Ω) is the measured resistance, Surf (cm²) the surface of the immersed plate, l (cm) the plate thickness. The plate was far enough from the electrodes so as to consider the potential uniform on its immersed surface; aCSF resistivity was neglected.

3.2. Results

The meter reached its saturation level, which means that the actual resistance was over $20 \text{ M} \cdot \Omega$. This corresponds to a resistivity of more than $2500 \text{ M} \cdot \Omega \text{ cm}$, or a conductivity of less than $4 \times 10^{-8} \text{ S} \cdot \text{m}^{-1}$. This is several orders of

magnitude higher than skull resistivity, which is in the range of 1–20 k Ω cm (Law, 1993). The measured resistance of aCSF alone was 79 Ω , which confirmed that it is negligible compared to that of methacrylate.

4. Main study: methods and materials

4.1. Visualization of defects

A burr hole that has been left open after surgery produces a high intensity signal characteristic of soft tissues on T1-weighted magnetic resonance imaging (MRI). A methacrylate plug is more difficult to discriminate with MRI, because it leads to a low intensity signal that can be confused with that of skull. However, it produces a rupture in the bone marrow high intensity line when that is visible. Also, some assumptions can be made on the skull defects locations based, for example, on the skin flap, which is visible on a 3D skin reconstruction. Another helpful way to track skull defects is to perform a curvilinear reconstruction (Bastos et al., 1999) of the skull. Of course, skull defects are also very visible on computed tomography (CT) scans or plain X-ray films, but these are not always available. See Fig. 1 for an overview of the burr holes seen by MRI.

A resected brain area is clearly seen with MRI: it is filled with CSF and is of low intensity on T1-weighted images (Fig. 2).

4.2. Defect-free model

All the realistic BEM models in our study were created

with Curry V4 (Neuroscan Labs). They were based on the T1-weighted MRI scan of a patient presenting skull defects and a temporal-lobe resection. We used Curry's automatic segmentation of scalp, skull and brain boundaries, based on gray level thresholds. We manually modified these boundaries in order to build a model that does not take into account the defects. The lengths of the triangle sides were 12, 10 and 8 mm for scalp, skull and brain meshes, respectively. This produced meshes with 1742, 1668 and 2062 triangles, leading to a model with 2779 nodes. Enclosed conductivities were 0.33, 0.0042, 0.33 S \cdot m⁻¹ for scalp, skull and brain, respectively (Geddes and Baker, 1967).

4.3. Modeling of defects

We then modified the defect-free model in order to account for skull and brain defects. It is important to note that the BEM is limited in that it can only model closed surfaces. Also, there is a generally accepted 'rule of thumb' stating that two BEM surfaces should not be closer than half their mesh triangle size: this implies that a local mesh refinement is needed when surfaces are too close to one another.

In the first category of burr hole model, we joined the brain and skull BEM surfaces at the level of the hole. We obtained one BEM surface only, which enclosed the remaining intact skull. The hole was placed at the vertex of the head in order to have a simple geometry in terms of skull conformation and electrode positions around the hole. This was the 'open burr hole' model (see Fig. 3a for a schematic representation of an equivalent spherical model, Fig. 4a for

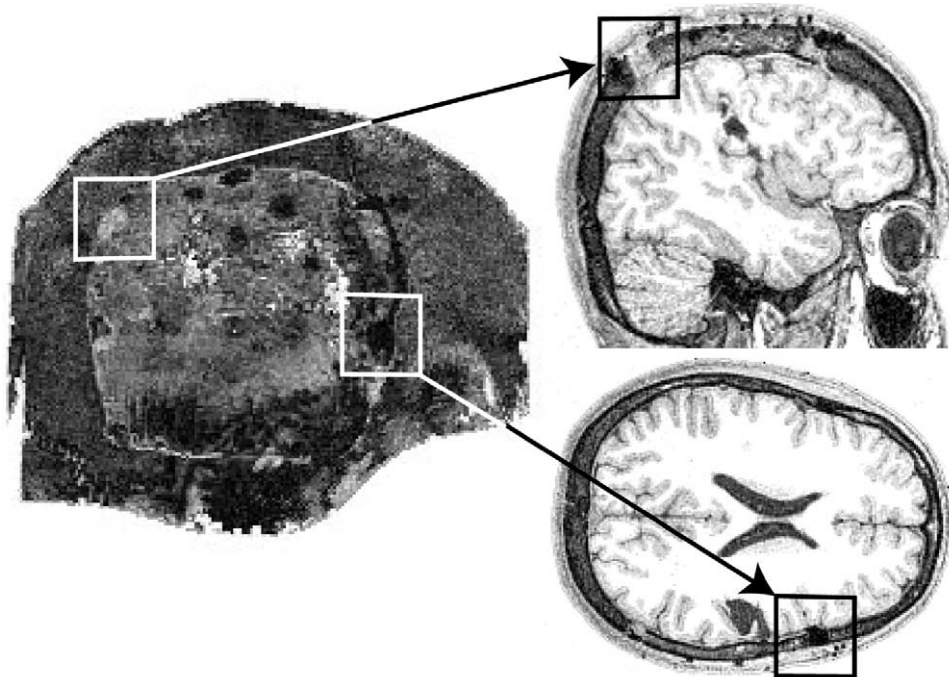


Fig. 1. Burr holes as seen with T1-weighted MRI: (left) reconstruction of an image along a curved surface following the skull (Brainsight software); (upper right) open burr hole; (lower right) burr hole that has been filled with methacrylate.

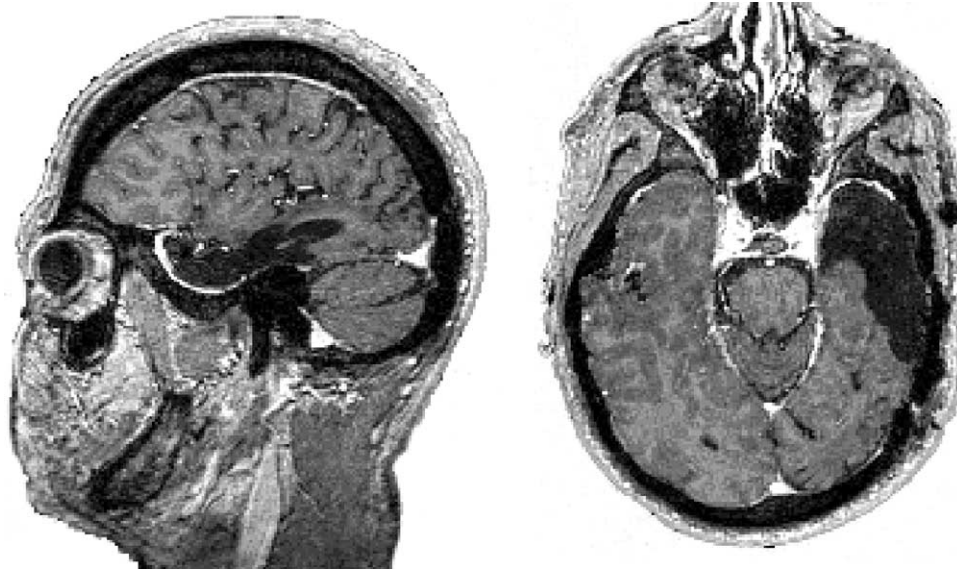


Fig. 2. Sagittal (left) and transverse (right) views of a temporal brain resection seen with T1-weighted MRI.

a view of the mesh). We also created a model with a hole at the location of the real burr hole in our reference patient in order to quantify the influence of the location of the hole. This was the ‘parietal burr hole’ model. In a second category of models, the hole was represented by a depression in the skull boundary. This type of model is a classical 3-layer model that was used as a reference in the validation of the less typical full hole model. Care was taken that skull and

brain boundaries did not get closer than 1 mm. This was insured by expanding the brain BEM surface with morphological tools in order to delineate the base of the depression. The skull thickness was approximately 7 mm in the region of the depression, the depth of which was 6 mm as a consequence. This was the ‘partial burr hole’ model (Fig. 3b). For all models, the skull BEM mesh was generated with a 10 mm triangle size and a 1.5 mm refinement in the area of the hole. Brain and scalp meshes were also refined around the defect.

The methacrylate plug was modeled as a small cylinder with near zero conductivity ($10^{-10} \text{ S} \cdot \text{m}^{-1}$). It was placed at the vertex of the head, between the skull and scalp surfaces (Fig. 3c). In a similar way as for the open burr hole, we used morphological tools to depress the scalp surface by 1 mm and expand the brain surface by 1 mm in order to delineate the top and bottom surfaces of the cylinder, the height of which was consequently around 5 mm. We used a 3 mm mesh.

The temporal-lobe resection was modeled with 6 mm-sided triangles, producing a surface enclosing 30 ml of CSF (conductivity of $1 \text{ S} \cdot \text{m}^{-1}$) (Figs. 3d and 4b).

4.4. Quantifying the influence of the defects

We placed a set of radial dipoles in the vicinity of each defect: below and lateral to the burr holes (Fig. 5a), behind and above the resection (Fig. 5b). For each dipole, we simulated the potentials that it would produce at 71 locations (10/10 system) on the surface of the realistic head model including the defect (see above Section 4.3). Then, a dipole was fitted on these potentials in the defect-free head model, using Curry’s simplex method and constraining the sources to be at least 3 mm away from the innermost BEM surface. We measured the resulting error in location and amplitude.

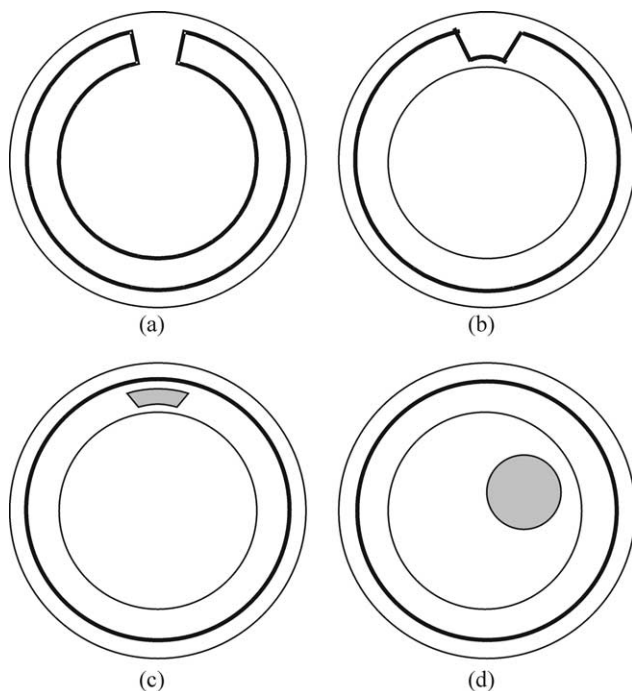


Fig. 3. Schematic views of the different types of models. The outer circle represents the skin surface, the thick line represents the skull, the inner circle the brain. (a) Full hole, (b) partial hole, (c) methacrylic plug, (shaded area) and (d) temporal resection (shaded area).

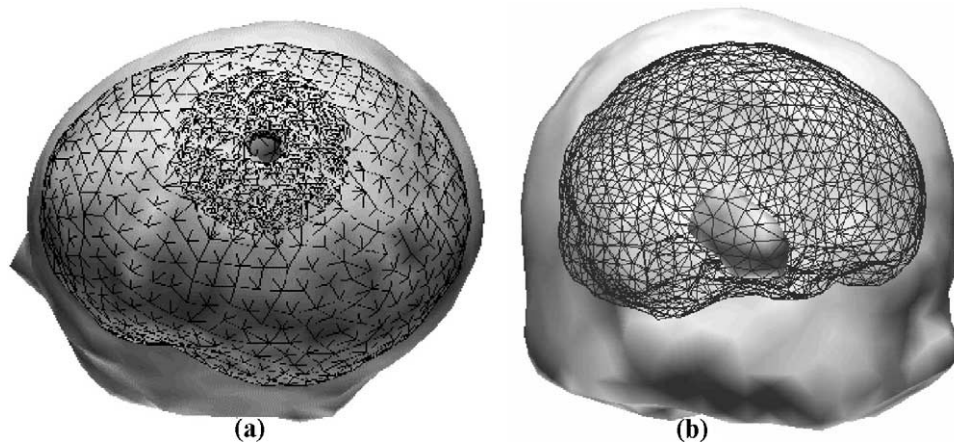


Fig. 4. BEM models (a) central hole and (b) temporal resection.

In order to validate our hole models, we also reproduced the experimental settings of van den Broek et al. (1998) and Thevenet et al. (1992). These studies used the FEM and were therefore not subject to some of the limitations of the BEM that are discussed below. In the first setting, we used a model with a full hole at a 60° elevation and dipoles on the z -axis (90° elevation). We computed the RDM (van den Broek et al., 1998) between the potentials computed with and without the hole. In the second setting, the hole was central and tangential dipoles were placed at different elevations; we simulated tangential dipoles in a full hole model and localized them without the hole. In the two experiments, meshes were refined around the hole and the dipoles.

4.5. Influence of noise on localization error

The methods we presented in the previous sections assume a noise-free environment. A more realistic configuration needs to take noise into account. We wanted to test (a) if the noise-free localization error is a good measure of

the mean error in a noisy situation and (b) if the variance of the localization error is similar when using either defect or defect-free model. We used the potentials created by a dipole located 20 mm below the skull in the central partial hole model. We added to the signal at each electrode one realization of a gaussian noise process. The amplitude of the noise was chosen so as to produce a signal to noise ratio (SNR) of 10. Then a dipole was fitted on these potentials with the defect-free head model, as in Section 4.3. We repeated the simulation 100 times, and computed the mean and standard deviation of the localization error, in both defect and defect-free configurations.

4.6. Use of different conductivities

Some authors (van Burik and Peters, 2000b; Cuffin et al., 2001) have suggested that skull conductivity may be higher than the classical value of $1/80$ times the scalp conductivity. We performed again the burr hole simulations with a skull conductivity of $1/40$ times the scalp value in order to assess the influence of skull conductivity on the reconstruction

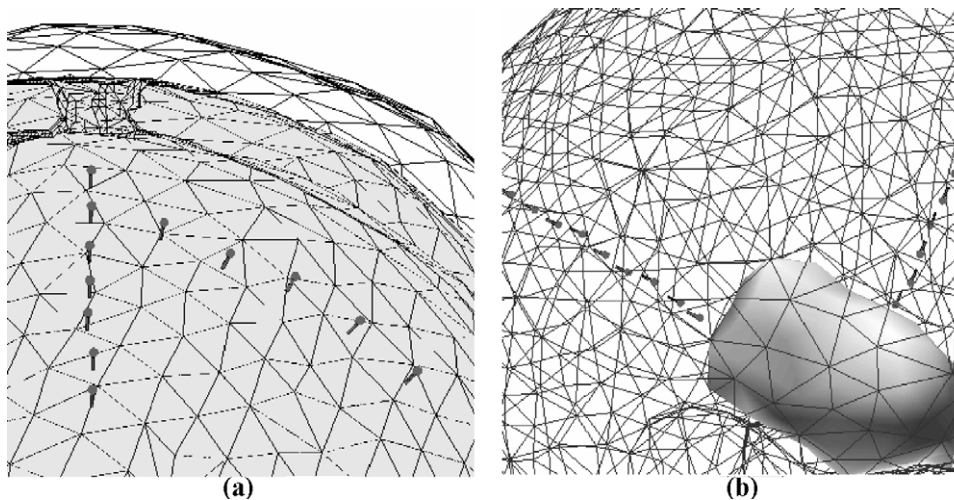


Fig. 5. (a) Dipoles below and lateral to hole. (b) Dipoles behind temporal resection.

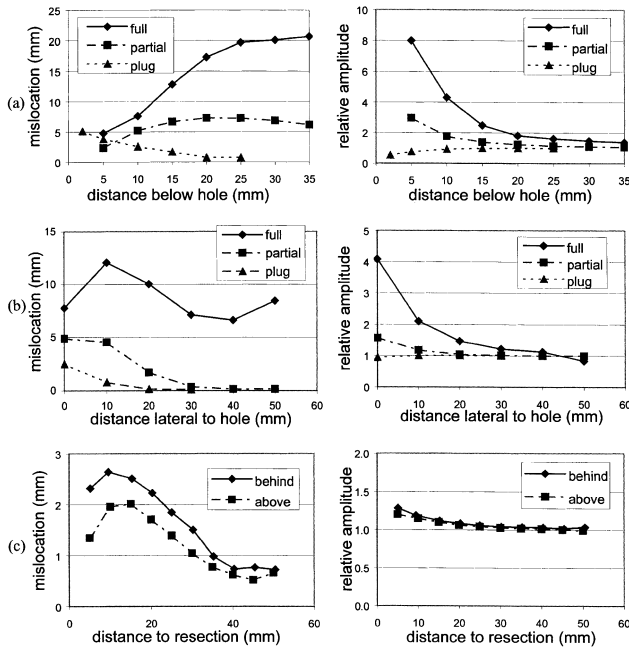


Fig. 6. Charts of errors in localization and amplitude. (a) Radial dipoles below central burr hole. (b) Radial dipoles lateral to central burr hole. (c) Dipoles behind and above temporal resection.

error. The CSF conductivity at body temperature may also be higher than the classical value of $1 \text{ S} \cdot \text{m}^{-1}$: Baumann et al. (1997) recommend a value of $1.79 \text{ S} \cdot \text{m}^{-1}$. We ran again the resection simulations with a value of $2 \text{ S} \cdot \text{m}^{-1}$.

5. Results

5.1. Open burr hole

Radial dipoles below the full hole were all reconstructed closer to the defect. For an original dipole between 5 mm and 20 mm below the hole, the fitted dipole was found as close to the hole as was permitted by our settings. For dipoles between 25 mm and 35 mm deep, the location error was of the order of 20 mm. The relative amplitude reached a maximum for dipoles just below the hole: 8 for a dipole 5 mm deep. It decreased exponentially with depth, and went below 1.5 at a depth of 30 mm. See Fig. 6a for an overview of the results. Radial dipoles lateral to the full hole were reconstructed closer both to the hole and to the surface. Location errors were of the order of 6–15 mm. The relative amplitude went below 1.5 at a distance of 20 mm from the hole (Fig. 6b).

The use of a partial central hole model lead to results with the same trend, but with much less extent. Indeed, the maximum location error was around 7 mm for a dipole 20 mm deep and the relative amplitude was of the order of 3 for a dipole 5 mm deep (Figs. 6a, b). In the partial parietal hole case, the amplitude factor was very similar to the central hole results, ranging from 1.1 to 2.7. However, the effect on

location error was somewhat smaller: errors ranged from 3.5 mm to 5.5 mm, with a peak when the dipole is at a depth of 15 mm only (results not shown).

In the two sets of simulations similar to van den Broek et al. (1998) and Thevenet et al. (1992), the results were in most cases very close to the corresponding FEM results obtained by these authors (Figs. 7 and 8, respectively). In the first study, though, the RDM values for the radial dipoles close to the surface was much higher than in van den Broek et al. (1998): for the dipole at 3 mm below the hole, we obtained 181% instead of 40% (Fig. 7b). We also noticed in the second study a tendency for dipoles to be reconstructed closer to the surface than in Thevenet et al. (Fig. 8); this was strongly reduced by a local refinement of the mesh around the dipoles.

5.2. Burr hole filled with methacrylate

In the case of the methacrylate plug model, radial dipoles were reconstructed further from the holes than their original location, with a location error and relative amplitude of 5 mm and 0.5 for a dipole 3 mm below the plug (Fig. 6a). For the dipoles lateral to the defect, the effect was significant

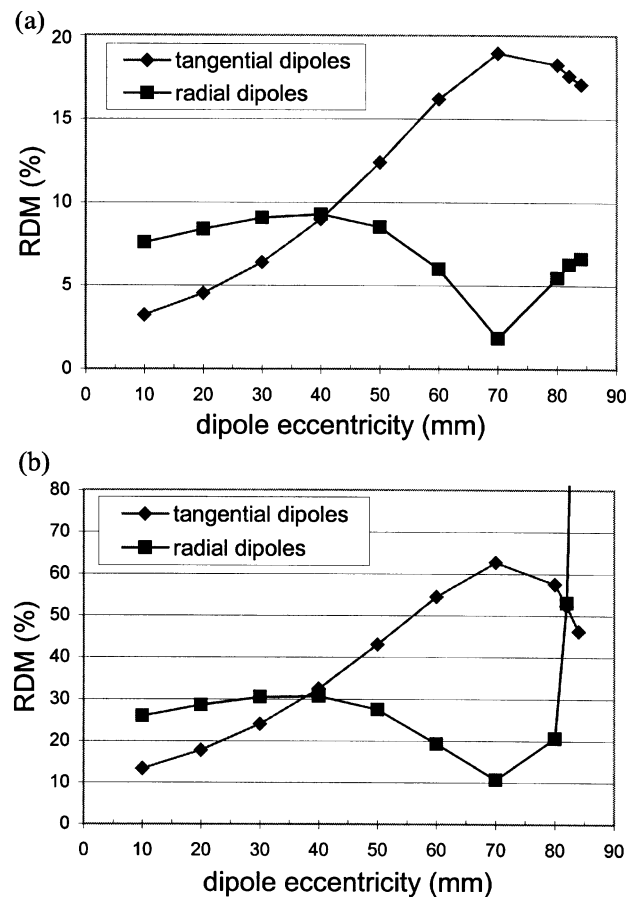


Fig. 7. RDM between potentials in the central hole models and the defect-free one for dipoles at given locations; (a) partial hole, (b) full hole (the value at eccentricity 84 mm is 181%, not shown).

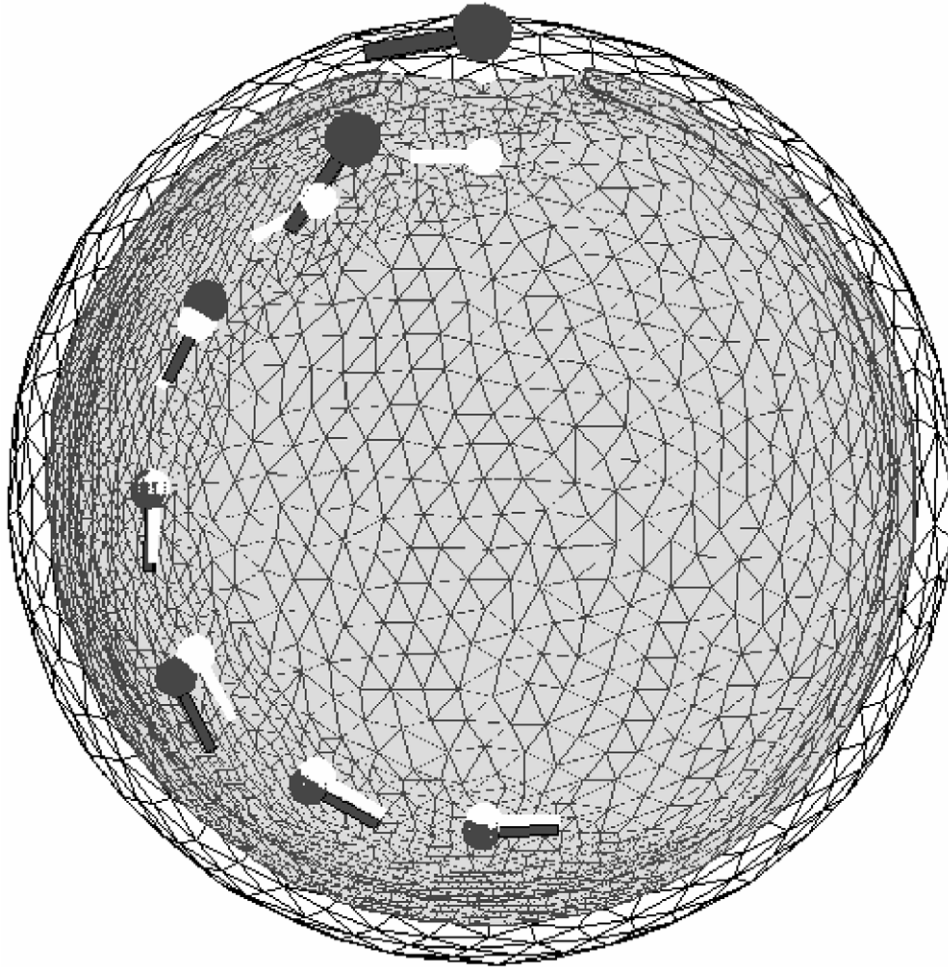


Fig. 8. Original dipoles in a full hole model (light gray) and dipoles reconstructed with the defect-free model (dark gray).

(more than 3 mm of location error) only in a radius of about 10 mm around the center of the plug (Fig. 6b).

5.3. Brain resection

The resection had a small effect on the dipoles placed behind and above it: the maximum localization error was less than 3 mm and the relative amplitude less than 1.3 (Fig. 6c).

5.4. Simulations with noise

The mean and standard deviation of localization error for the 20 mm deep dipole simulated with the partial hole model and reconstructed using the same model were 2.7 ± 1.3 mm (see Fig. 9 for a histogram of the location error). This corresponds to the effect of the noise alone. When the defect-free model was used for localization, they were 7.2 ± 1 mm, reflecting the effect of the partial hole in the context of noise (to be compared to the value of 7.24 mm in a noiseless situation, cf. Fig. 6a). We have to note the presence of outliers that probably correspond to

instabilities in our models and were not included in our statistics (Fig. 9).

5.5. Use of different conductivity values

When full hole models with higher skull conductivity were used, we obtained location errors of $78 \pm 17\%$ and a

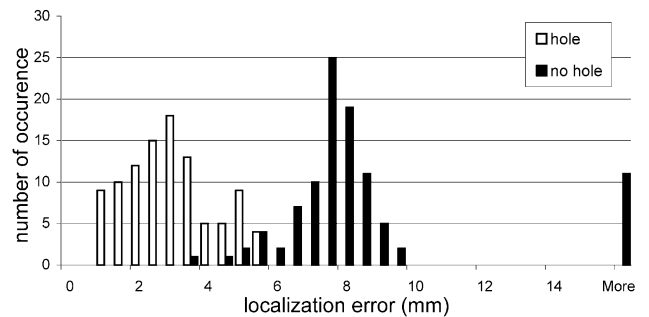


Fig. 9. Histograms of localization error for dipoles simulated in the partial hole model and reconstructed in a noisy environment with a model that includes the hole (light bars) or not (dark bars). Note the outliers at the right of the graph when the hole is not included.

relative amplitude of $73 \pm 9\%$ of the ones with a classical conductivity. In the partial hole models, the ratios were $88 \pm 7\%$ and $94 \pm 5\%$, respectively. Errors caused by burr holes were therefore smaller in the context of higher bone conductivity.

In the resection simulations, the use of a CSF conductivity of $2 \text{ S} \cdot \text{m}^{-1}$ lead to a maximum localization error of 3.5 mm for a dipole 10 mm behind the resection and a maximum amplitude factor of 1.4 for a dipole 5 mm behind the resection. This corresponds, respectively, to 31% and 8% more than the results for the classical value.

6. Discussion

We have shown in this paper that post-surgical burr holes have a significant effect on EEG and dipole localization, in concordance with previous studies (Thevenet et al., 1992; van den Broek et al., 1998; Vanrumste et al., 2000). If holes were not included, large errors in location and amplitude were obtained when reconstructing sources located near the defects, as expected. A quantitative evaluation of the impact of omitting the full hole leads to values generally similar to the ones of previous FEM studies (Thevenet et al., 1992; van den Broek et al., 1998), with some important variations though. Indeed, the impact of omitting the hole was much larger than in van den Broek et al. (1998) for dipoles very close to the surface. This is probably due to the typical instability for dipoles close to BEM surfaces, and could possibly be reduced by an even finer mesh. Also, dipoles very far from the hole are reconstructed closer to the surface, contrary to Thevenet et al. (1992). This could be due to the well-known numerical error resulting from a low-conductivity skull layer in the BEM, which cannot be minimized here by the isolated problem approach (IPA), because the latter requires concentric layers (see for example Meijs et al., 1989). This effect seems to be more pronounced in the lower part of the sphere – probably because we are dealing with smaller values that are more affected by numerical errors. Nevertheless, it is important to note that BEM results were close to the FEM results for dipoles in the regions where currents sources are likely to be located (more than 5 mm away from the skull and in the middle and upper parts of the sphere). The fact that errors were reduced by a higher mesh refinement emphasizes again the importance of refining the meshes in the region of the dipoles. We found an influence of the hole location, parietal or central, as in van den Broek et al. (1998), but it was quite limited.

We demonstrated that the more numerous methacrylic plugs also had an influence on dipole localization, suggesting that they should be taken into account when sources are near the plug and precision is sought. The situation was quite different for the temporal CSF-filled cavity: it produced little effect on dipole modeling despite its large size and can therefore be omitted without much consequence. This is in discordance with van den Broek et al.

(1998) and Vanrumste et al. (2000) who had both studied the impact of the CSF-filled ventricular system. This discrepancy may be due to the relative position of the dipoles, the CSF cavity and the electrodes. Indeed, in Vanrumste et al. (2000) the dipoles that are more affected by the cavity are the ones located beneath it, i.e. the ones for which the cavity stands between the dipole and a large number of electrodes. In our simulations the cavity lies on the side of the dipoles and possibly produces less interference on the measured potentials, as it has an important effect on a small number of electrodes.

We studied the localization errors in a noisy environment, and verified that the mean dipole was close to the one reconstructed in a noise-free setting. This suggests that we can use the error value encountered in a noise-free environment as a measure of a ‘mean’ localization error that would be obtained with noise. The error variance was similar in the defect and defect-free situations. We have to note the presence of instabilities in the fitted dipoles in the noisy situation (outliers). This suggests again that one has to be particularly cautious when using complex BEM models. We ran again the noise-free simulation studies in the context of doubled skull and CSF conductivity and found only a small impact on the resulting errors.

All our models comprised 71 electrodes, which represent a high spatial sampling. In a clinical setting, the lower number of electrodes is typically of the order of 30. This will almost certainly lead to localization errors due to spatial aliasing on top of the errors coming from not considering the defects. As the potential gradients are stronger in the case of a skull hole (i.e. higher spatial frequency content), the aliasing is expected to be stronger, emphasizing the need for high spatial sampling around the hole (Bénar and Gotman, 2001).

We used BEM models in all our EEG studies, which can only handle closed surfaces that are not in contact with one another. This is a limitation in modeling defects, for example, with methacrylate plugs or multiple holes. Some investigation should therefore be conducted in order to assess the advantage in our context of using the more computationally demanding FEM, which does not have this limitation, and in the context of magnetoencephalography, which is not significantly influenced by the skull. Nevertheless, we have found the largest effect for the open burr hole, which can be easily modeled when unique (the most common case). Therefore, EEG modeling using BEM remains a valuable tool in the study of post-operative epileptic patients.

Acknowledgements

We would like to thank the reviewers for their very useful comments, as well as Dr Aviva Abosh for her input on epilepsy surgery and Dr André Leduc for his help in measuring methacrylate conductivity. This research was supported in part by grant MT-10189 of the Canadian Institutes of

Health Research and in part by a Natural Science and Engineering Research Council studentship.

References

- Barnard AC, Duck IM, Lynn MS, Timlake WP. The application of electromagnetic theory to electrocardiology. II. Numerical solution of the integral equations. *Biophys J* 1967;7:463–491.
- Bastos AC, Comeau RM, Andermann F, Melanson D, Cendes F, Dubeau F, Fontaine S, Tampieri D, Olivier A. Diagnosis of subtle focal dysplastic lesions: curvilinear reformatting from three-dimensional magnetic resonance imaging. *Ann Neurol* 1999;46:88–94.
- Baumann SB, Wozny DR, Kelly SK, Meno FM. The electrical conductivity of human cerebrospinal fluid at body temperature. *IEEE Trans Biomed Eng* 1997;44:220–223.
- Bénar CG, Gotman J. Non-uniform spatial sampling in EEG source localization. *Proceedings of the 23rd International Conference of the IEEE Engineering in Medicine and Biology Society*; 2001 in press.
- Berger H. Hans Berger on the electroencephalogram of man (translated by P. Gloor). *Electroenceph clin Neurophysiol* 1930(Suppl 28):48.
- van den Broek SP, Reinders F, Donderwinkel M, Peters MJ. Volume conduction effects in EEG and MEG. *Electroenceph clin Neurophysiol* 1998;106:522–534.
- van Burik MJ, Peters MJ. EEG and implanted sources in the brain. *Arch Physiol Biochem* 2000a;107:367–375.
- van Burik MJ, Peters MJ. Estimation of the electric conductivity from scalp measurements: feasibility and application to source localization. *Clin Neurophysiol* 2000b;111:1514–1521.
- Cobb WA, Guiloff EJ, Cast J. Breach rhythm: the EEG related to skull defects. *Electroenceph clin Neurophysiol* 1979;47:251–271.
- Cuffin BN. Effect of local variations in skull and scalp thickness on EEG's and MEG's. *IEEE Trans Biomed Eng* 1993;40:42–48.
- Cuffin BN, Schomer DL, Ives JR, Blume H. Experimental tests of EEG source localization accuracy in spherical head models. *Clin Neurophysiol* 2001;112:46–51.
- Geddes LA, Baker LE. The specific resistance of biological materials – A compendium of data for the biomedical engineer and physiologist. *Med Biol Eng* 1967;5:271–293.
- Hämäläinen MS, Sarvas J. Realistic conductivity geometry model of the human head for interpretation of neuromagnetic data. *IEEE Trans Biomed Eng* 1989;36:165–171.
- Kavanagh RN, Darcey TM, Lehmann D, Fender DH. Evaluation of methods for the three-dimensional localization of electrical sources in the human brain. *IEEE Trans Biomed Eng* 1978;BME-25:421–429.
- Law SK. Thickness and resistivity variations over the upper surface of the human skull. *Brain Topogr* 1993;6:99–109.
- Marin G, Guerin C, Baillet S, Garnero L, Meunier G. Influence of skull anisotropy for the forward and inverse problem in EEG: simulation studies using FEM on realistic head models. *Hum Brain Mapp* 1998;6:250–269.
- Meijs JWH, Weier OW, Peters MJ, Van Oosterom A. On the numerical accuracy of the boundary element method (EEG application). *IEEE Trans Biomed Eng* 1989;36:1038–1049.
- Nunez PL. *Electrical fields of the brain*, New York, NY: Oxford University Press, 1981.
- Olivier A. Commentary: cortical resections. In: Engel Jr J, editor. *Surgical treatment of the epilepsies*, New York, NY: Raven, 1987. pp. 405–416.
- Ollikainen JO, Vauhkonen M, Karjalainen PA, Kaipio JP. Effects of local skull inhomogeneities on EEG source estimation. *Med Eng Phys* 1999;21:143–154.
- Rush S, Driscoll DA. EEG electrode sensitivity – an application of reciprocity. *IEEE Trans Biomed Eng* 1969;BME-16:15–22.
- Thevenet M, Bertrand O, Perrin F, Pernier J. Finite element method for a realistic head model of electrical brain activities. *Proceedings of the 14th International Conference of the IEEE Engineering in Medicine and Biology Society, Satellite Symposium on Neuroscience and Technology*, Lyon, 1992. pp. 2024–2025.
- Vanrumste B, Van Hoey G, Van de Walle R, D'Havé M, Lemahieu I, Boon P. Dipole location errors in electroencephalogram source analysis due to volume conductor model errors. *Med Biol Eng Comput* 2000;38:528–534.
- Yan Y, Nunez PL, Hart RT. Finite element model of the human head: scalp potentials due to dipole sources. *Med Biol Eng Comput* 1991;29:475–481.